WEP Warwick Evans Publishing

International Journal of Materials Science and Technology Studies

ISSN: 3006-7693 (Print), ISSN: 3006-3744 (Online) | Volume 5, Number 1, Year 2026
DOI: https://doi.org/10.62051/ijmsts.v5n1.02
Journal homepage: https://wepub.org/index.php/IJMSTS/index

A Review of the Application of Covalent Organic Frameworks in Uranium Extraction from Seawater

Minghao Guo [1, *], Yibo Wang [2], Meiyi Li [1], Jiazheng Tian [1]

[1] College of Environmental Science and Engineering, North China Electric Power University, Beijing 102206, P.R. China

[2] College of Chemistry and Chemical Engineering, University of South China, Hengyang, Hunan 421001, P.R. China

*Corresponding Author: guominghao0026@163.com

ABSTRACT

The ocean contains abundant uranium resources. From the perspectives of resource utilization and ecological environmental protection, uranium extraction from seawater represents a highly promising method for uranium resource regeneration. This approach holds significant potential for the advancement of nuclear power and the broader application of reliable energy. Covalent organic frameworks (COFs) are ideal materials for extracting U(VI) ions from seawater due to their inherent porosity, robust skeletal structure, chemical stability, and good structural regularity. This paper reviews recent progress in the efficient preconcentration and separation of U(VI) from seawater through adsorption and photocatalysis. The current developments and potential of U(VI) extraction using functional COFs are also discussed. Lastly, this review highlights the opportunities and challenges associated with COF-based seawater uranium extraction, offering insights into its future development prospects. This work aims to deepen readers' understanding of the key technologies involved in COFs for seawater uranium extraction, and to identify more efficient and environmentally friendly COF-based materials, thereby supporting the growth of the nuclear power industry.

KEYWORDS

Uranium; Covalent organic frameworks; Seawater; Adsorption; Photocatalysis

1. INTRODUCTION

Rising global energy demand and fossil fuel pollution urge sustainable alternatives. Nuclear power is promising, yet surging uranium demand and finite terrestrial reserves, sufficient for only about 100 years of use, make exploring new uranium resources imperative [1-6].

At present, the technical methods of extracting uranium from seawater mainly include adsorption, photocatalysis [7-11]. Over the years, researchers have developed a variety of materials for the adsorption of U(VI), such as metal-organic framworks (MOFs) [12, 13], porous aromatic frameworks (PAFs) [14, 15], and porous organic polymers (POPs) [16-18]. PAFs have some limitations, including poor thermal and chemical stability [19], and the structure order of POPs is not high, which leads to a decrease in the adsorption efficiency of U(VI) [20]. However, despite their regular porosity and good crystallinity, the stability of MOFs when used in extreme conditions is still a great challenge [21]. COFs have several significant advantages, including a highly ordered crystalline structure, high specific surface area, adjustable pore size, diversity of functional groups, and good chemical stability [22-25]. Therefore, COFs has good development prospects in adsorption reduction [26], gas storage and separation [27], catalyst carrier [28], photoelectric catalysis, and other aspects. Since the first

discovery of COFs by Yaghi and colleagues in 2005 [29], a growing number of research and reports have been devoted to discovering the properties and uses of this innovative material. COFs combine conventional nanomaterial properties with unique merits: tunable crystalline structures and pore sizes [30-33], superior environmental stability [34-36], large specific surface area for enhanced adsorption and catalysis, and low light-element-based density enabling high adsorption capacity [37-41]. As an emerging organic framework, COFs feature high porosity, ordered channels and good chemical stability, serving as promising porous materials. Their large surface area, rich active sites and high stability suit catalytic applications well. Studies show radionuclide extraction from complex solutions relies heavily on adsorbent properties, particularly selective U(VI) capture via tailored functional groups, pore sizes and active sites [42].

Seawater uranium extraction traces back to Davies et al.'s 1964 proposal. Late 1990s Japanese studies yielded amidoxime nonwovens that extracted ~1 kg uranium from seawater. In 2019, the U.S. Department of Energy review spurred new adsorbent research, exemplified by Li et al.'s CMM composite with a 582.46 mg/g maximum U(VI) adsorption capacity [43]. A graphene oxide-based functional chitosan hydrogel was prepared and applied to the adsorption of uranium in seawater by Wen et al. After 14 days of adsorption in native seawater, the adsorption amount of the hydrogel reached 9.2 mg/g. In 2020, tang et al. summarized the synthesis and application of xiamidoxime based adsorbent for U (VI) extraction in seawater [44]. In a summary of the purification of U(VI) containing wastewater and discussed the relationship between the material type and the adsorption mechanism, Jun et al. [45] and Ma et al. [46] summarized the removal of U(VI), including biotechnology, membrane separation, adsorption, precipitation, ion exchange, and photocatalysis.

However, COFs-based U(VI) adsorption and photocatalysis for seawater separation remain rarely reported. This review summarizes recent advances in COFs-based seawater U(VI) extraction, covering adsorptive and photocatalytic applications, and discusses performance-enhancing strategies.

2. EXTRACTION OF URANIUM BY COFS

Uranium (U, atomic number 92) comprises three long-lived radioactive isotopes, with ^{235}U as the only natural fissile nuclide (≈195 MeV/fission) and ^{238}U critical for plutonium production [47-50]. In aqueous phases, U exists as stable linear UO_2^{2+} ions, which act as hard acids favoring oxygen-donor over nitrogen-donor coordination [51-52]. Seawater U occurs primarily as $Ca_2[UO_2(CO_3)_3]$ complexes, with a low concentration (3.3 μg/L), but total reserves of 4.5 billion tons (1000 × terrestrial levels) [53]. Common seawater U recovery strategies include solvent extraction, ion exchange, membrane filtration and biosorption [54].

2.1. COFs as Adsorbents for Seawater Uranium Extraction

There are two main adsorption mechanisms between COFs and U(VI). First, COFs materials act as adsorbents, and the functional groups in the materials coordinate with uranyl, forming a stable chemical bonding. The other is COFs materials act as photocatalytic catalyst to reduce uranyl through redox [55].

2.1.1. Original COFs

COFs are advanced porous crystalline materials featuring the precise incorporation of diverse functionalized moieties, ordered periodic arrays, whose modular structure and extremely extensive chemical and reticular topological changes can be translated into tunable properties. Zhang et al. [56] designed a new two-dimensional microporous phosphoritrile MPCOF using trihexachlorocylic triphospitrile (HCCP) and hydrophenylenediamine (PDA) as raw materials. In the adsorption experiment of simulating uranium in spent fuel, MPCOF showed the maximum U(VI) adsorption capacity under weak acidic conditions (pH=4.5), with an adsorption capacity of 169 mg/g and a selectivity of 76 % (Figure 1a). Under the strong acid conditions, the adsorption capacity of U(VI)

has decreased (Figure 1b). However, kinetic studies show that the material adsorption process takes 3 weeks or more to reach equilibrium, with the slow adsorption process attributed to the lower surface area of MPCOF and smaller total pore volume (Figure 1c), limiting the amount of U(VI) diffusion into MPCOF through the ultrahole. Zhang et al. [57] reported a double-ring pore Dp-COF, which has a mean-ring tricarboxylic acid group towards the center and can construct a unique double ringstructure. The inner pore is formed by hydrogen bonds, which facilitates the size matching adsorption of COFs and target ions. Under the high acidity of pH=1.0, the adsorption amount of Dp-COF can still reach 66.3 mg/g. Moreover, the adsorption of Dp-COF to uranium gradually increased with increasing pH, reaching a maximum value of 317.3 mg/g at pH=4.5 (Figure 1d). The reason is that due to the unique double-ring pore structure of Dp-COF, the diameter of the hydrated uranyl ion is closest to that of Dp-COF (other smaller metal ions can easily pass through the inner pore of Dp-COF, without this size effect), and this physical effect is usually not susceptible to protonation in acidic solution. Thus, Dp-COF material has better adsorption performance on uranium in simulated seawater solution. The target size matching effect of Dp-COF inner pore doubling was more significant at low concentration. As shows that the uranium removal rate by Dp-COF is very high, up to 99.8 %, at an initial uranium concentration of 20 mg/L (Figure 1e). In the multi-ion system under the same conditions, the adsorption amount of Dp-COF can reach 0.26 mmol/g, and the selectivity can also reach 83.0 %, indicating that the unique two-ring pore structure of Dp-COF shows stronger specificity and affinity for uranium, thus greatly improving the adsorption capacity and selectivity of the material for uranium (Figure 1f). The adsorption performance of COFs can also be improved by designing COFs materials to match specific metal ions. ACOF synthesized by Li et al. [58] has high crystallinity, good physical and chemical stability, and good adsorption performance for U(VI). Under high acidic conditions, the adsorption capacity of U(VI) decreased, but the adsorption selectivity was improved. Research shows that under the condition of high acid, hydrogenions strong protonation ACOF part of the ketone structure into enol structure, the coordination capacity of uranium and alcohol hydroxyl (C-OH) is weaker than with ketone (C=O), so the adsorption capacity of ACOF will decrease with the increase of acidity, but compared with the ketone, enol structure aperture is closer to the diameter of hydration U(VI) ion, make the size matching effect of adsorption process, thus improve the adsorption selectivity of uranium.

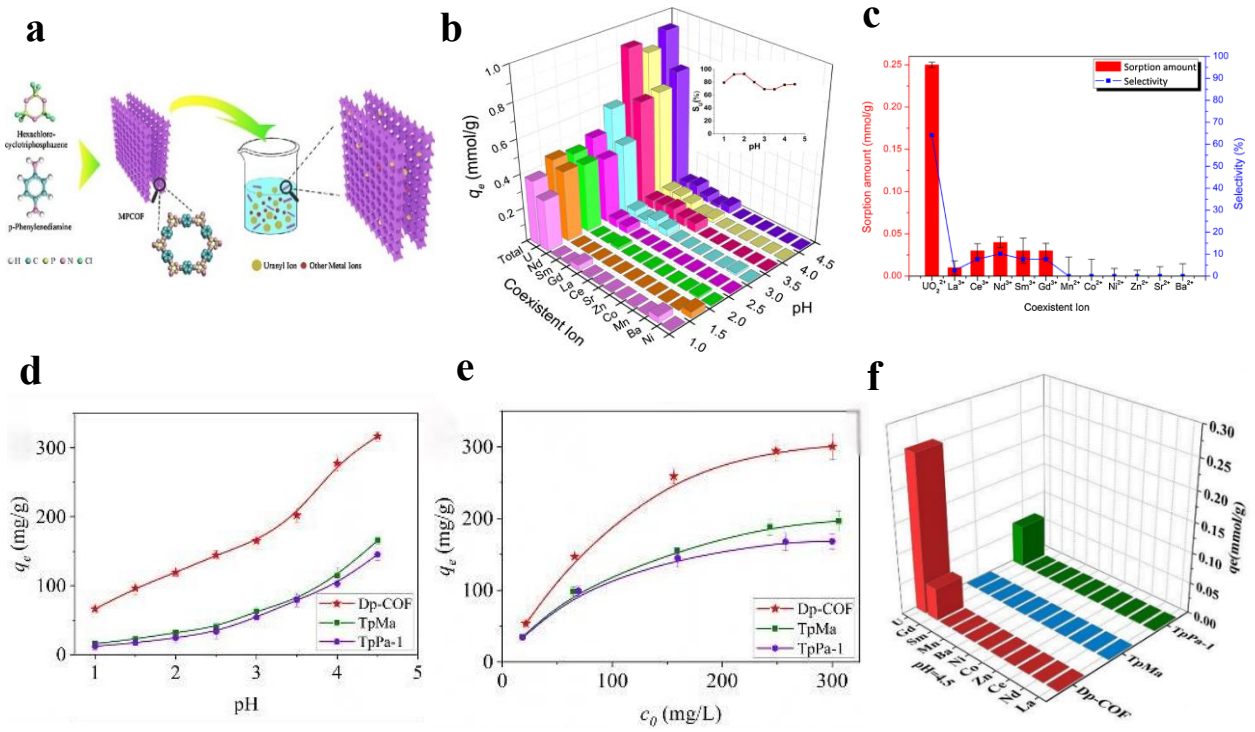

Figure 1. (a) The sorption modes for uranium onto MPCOF. (b) Effect of pH on the sorption capacity and selectivity (inset) of MPCOF towards U(VI) in simulated nuclear industry effluent. (c) Sorption capacity and selectivity for sorption of each metal ions onto MPCOF in strong acidic multi-ion system [56]. (d) Effect of pH on the adsorption for uranium. (e) Effect of inital uranium concentration on the adsorptio. (f) Effect of pH on the adsorption for each cation [57].

2.1.2. Functional group-modified COFs

Although traditional COFs can adsorb U(VI), it may have insufficient effects in adsorption efficiency, stability, and other aspects. To improve the adsorption properties of COFs as adsorbents, functional groups selectively coordinating with the target ions can be introduced for modification. For example, functional groups with excellent adsorption properties for U(VI), such as amidoxime (AO) [59, 60], carboxylate (-COOH) [44], and phosphoryl (-$PO(OH)_2$) etc. Li et al. [61] reported a new COFs based material (COF-COOH), COF-COOH adsorption of U(VI) ions mainly depends on the carboxyl adsorption and pore physical adsorption, in the adsorption rate is not perfect, so Li et al. functional group with 2-(2, 4-dihydroxyphenyl)-benzmi-azole (HBI) for COF-COOH, for uranium efficient new solid phase extraction agent (COF-HBI) (Figure 2a). The modified adsorption capacity of COF-HBI depends on the good coordination selectivity of HBI ligand and U (VI). Compared with COF-COOH, the uranium sorption selectivity of COF-HBI significantly increased in the simulated nuclearindustry effluent with 11 kinds of competing ions (Figure 2b). In the most favorable conditions, the equilibrium sorption capacity of COF-COOH for uranium could reach 211 mg/g (Figure 2c). Amidoxime (AO) is recognized as a modification method with high adsorption performance for U (VI). The study shows that the binding effect of AO and uranyl is easier thermodynamically and the strong chelation ability of AO (N and O atoms of AO and metal ions) are the key to achieve high adsorption performance. The COF-TpDb-AO prepared by Sun et al. [62] can rapidly adsorb 99.7 % uranium within 5min with a maximum adsorption of 408 mg/g (Figure 2d). It shows that the laminated sheet of COF-TpAb-AO behave as a stacked structure, providing continuous nanoscale channels perpendicular to the stacking direction, providing a path for ion transport (Figure 2e). In addition, the periodic arrangement of AO in COF-TpAb-AO also promotes the binding of the material to U(VI). Adding 20 μg/g of uranium to high ionic strength seawater can also reach 127 mg/g of adsorption amount (Figure 2f). In addition, it is worth mentioning that Li et al. [59] studied a series of sp^2, carbon conjugated COFs (COF-PDAN-AO, TP-TFCOF-BTAN-AO) were connected by carbon-carbon

double bonds (C=C) to avoid the main chain spatial arrangement. The distorted conformation facilitates the formation of in-plane π-conjugation and highly stable COFs structures. The abundant AO on the pore wall and the 1D channel for U(VI) provide the material with excellent selective separation of U(VI). Moreover, after the elution of Na_2CO_3, the material can still maintain good adsorption function after multiple cycles (6-9 times), which has higher reuse ability than other materials. Yu et al. [44] reported on the COF-IHEP-1 and COF-IHEP-2 for phosphoryl modification, it was the first U (VI) extraction of COFs from a highly acidic solution. The COF-IHEP-1 and COF-IHEP-2 structural units are connected by bonds to ensure the stability of the structure under highly acidic conditions, while the weak base of the bond weakens its ability to bind to protons, ensuring that it can have a negative electric or neutral surface at low pH, helping to trap uranyl ions from acidic solution (Figure 2g). Improving the overall structure selectivity due to the strong coordination ability between the phosphoryl group and uranyl. The adsorption amount of COF-IHEP-1 to U(VI) reaches 257 mg/g at pH=5, it is already higher than that of most reference materials under the same conditions. And it is worth noting that the adsorption capacity of COF-IHEP-1 to U(VI) retained 92 % adsorption capacity after four adsorption-desorption cycles (Figure 2h).

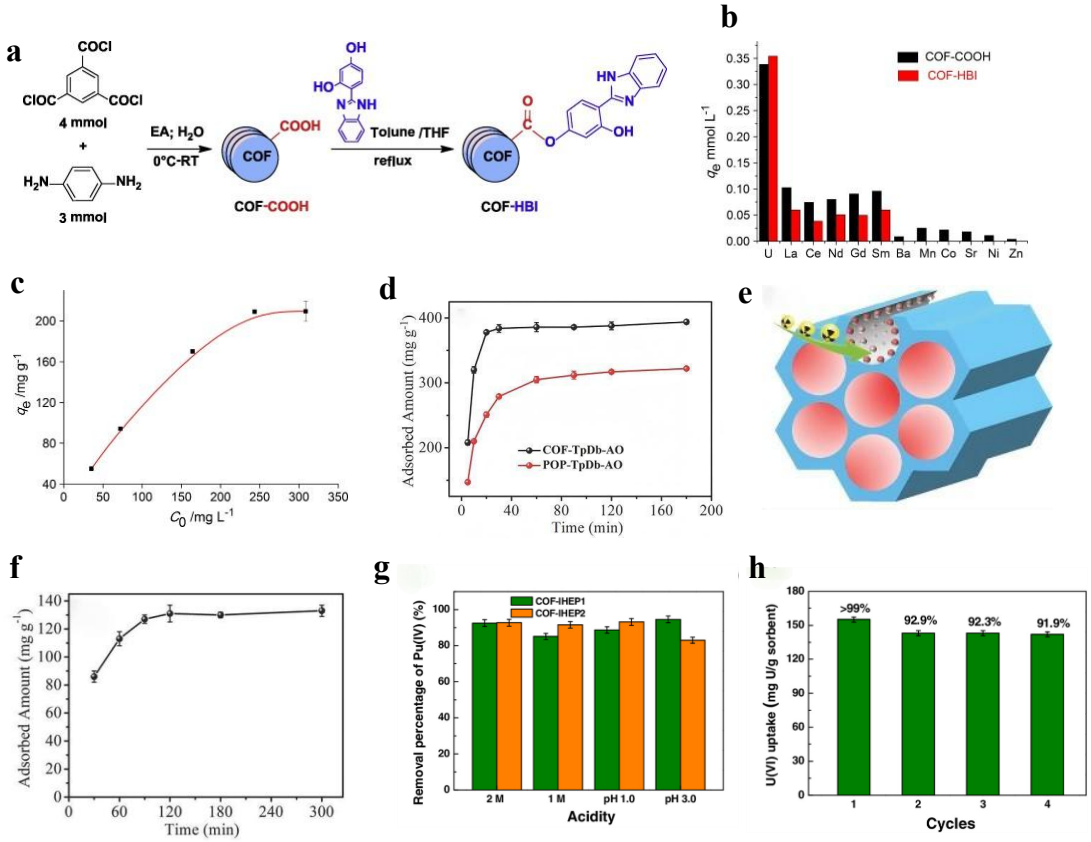

Figure 2. (a) Schematic illustration of the preparation of COF-COOH and COF-HBI. (b) Competitive adsorption capacities of coexistent ions on COF-COOH and COF-HB. (c) Equilibrium isotherm for the adsorption of U(VI) [61]. (d) The kinetics of uranium adsorption from aqueous solution with an initial concentration of 9.25 ppm (400 mL), at pH≈6, and adsorbent material (4.5 mg). (e) Schematic illustration of chelating groups in COFs. The uniform pore morphology of the COFs leads to the functionalized material with unrestricted access of ions to all of the chelating sites. (f) The kinetics of uranium adsorption from seawater spiked with 20 ppm uranium at a V/m=40000 mL/g [62]. (g) Removal percentage of Pu(IV) with COF-IHEP1 and COF-IHEP2 for a wide range of acidity. (h) Recycle use of COF-IHEP1 and COF-IHEP2 for U(VI) uptake at pH=1.0 [44].

2.1.3. COFs combined with other materials

There are always deficiencies in single COFs materials, such as the poor insolubility and dispersity of microcrystalline COFs powders in most solvents limiting their processing into useful practical products. Therefore, combining COFs with other materials with excellent adsorption properties and designing them into composite materials also means to optimize the adsorption properties. Reasonable design structure can retain the excellent properties of the two materials, while make up for some shortcomings of the two themselves, improve the overall performance of the materials, broaden the application field, and meet the diversified needs. Zhong et al. [39] combined COFs TpPa-1 with bimmanganese ore (δ-MnO_2) into δ-MnO_2@TpPa-1 (Figure 3a). Compared with δ-MnO_2, the specific surface area of the composite δ-MnO_2@TpPa-1 increases by 5-fold, the pore volume increases, and the pore diameter decreases. δ-MnO_2@TpPa-1 has good recycling activity and specific excellent development prospects in removing U(VI) (Figure 3b). Through infrared spectroscopy analysis and electron spectroscopy, it shows that δ-MnO_2@TpPa-1 provides greater active surface and better electrical conductivity in the adsorption process, and accelerates the electron transfer between the adsorbent and U(VI). Hydroxyapatite (HAP) has excellent adsorption capacity for U(VI), but external conditions and adsorption capacity and other factors will affect its adsorption efficiency. You et al. [63] doped hydroxyapatite (HAP) into a COF-based material (COF-COOH) to synthesize inorganic-organic porous skeleton composites (COF-HAP) (Figure 3c). The maximum adsorption capacity of U(VI) on the COF-HAP is 510 mg/g (Figure 3d). The study shows that the adsorption behavior of COF-HAP to U(VI) is complex, including the adsorption of carboxyl group to U(VI)through surface collaterals, the ionization of HAP in COF-HAP to produce a small amount of Ca(II) under acidic conditions, the fixation of U(VI)by surface precipitation, and the ion exchange between Ca(II) and U(VI). The combination of multiple actions makes COF-HAP have ultra-high adsorption capacity for U(VI). As an emerging organic-inorganic hybrid material, MOF materials have great potential in the field of adsorption. When MOFs were used in combination with COFs, the performance of the mixed material improved significantly compared to the composition alone. This combined strategy not only improves the stability of the adsorbent, but also improves the uranium removal efficiency to some extent. Liu et al. [29] used a mild hydrothermal method to recombine the water-stabilized MOFs material with highly crystalline COFs to synthesize a structurally stable and active functional group-rich advanced composite, UiO-66-NH_2@LZU1 (Figure 3e). The composite has both COFs and MOFs properties, it has higher stability, larger specific surface area and faster adsorption efficiency that cannot be impossible for a single component to achieve. The UiO-66-NH_2@LZU1 has the largest uranium adsorption capacity (180.4 mg/g), exceeding the UiO-66-NH_2 (108.8 mg/g) and COF-LZ1 (65.8 mg/g), achieving a good mixing effect (Figure 3f). Studies have shown that UiO-66-NH_2@LZU1 is rich in nitrogen (from COF-LZU1), and the oxygen (from UiO-66-NH_2) groups can bind to U(VI) to promote the removal of uranium. In addition, the electrostatic interaction is also a mechanism of the removal process.

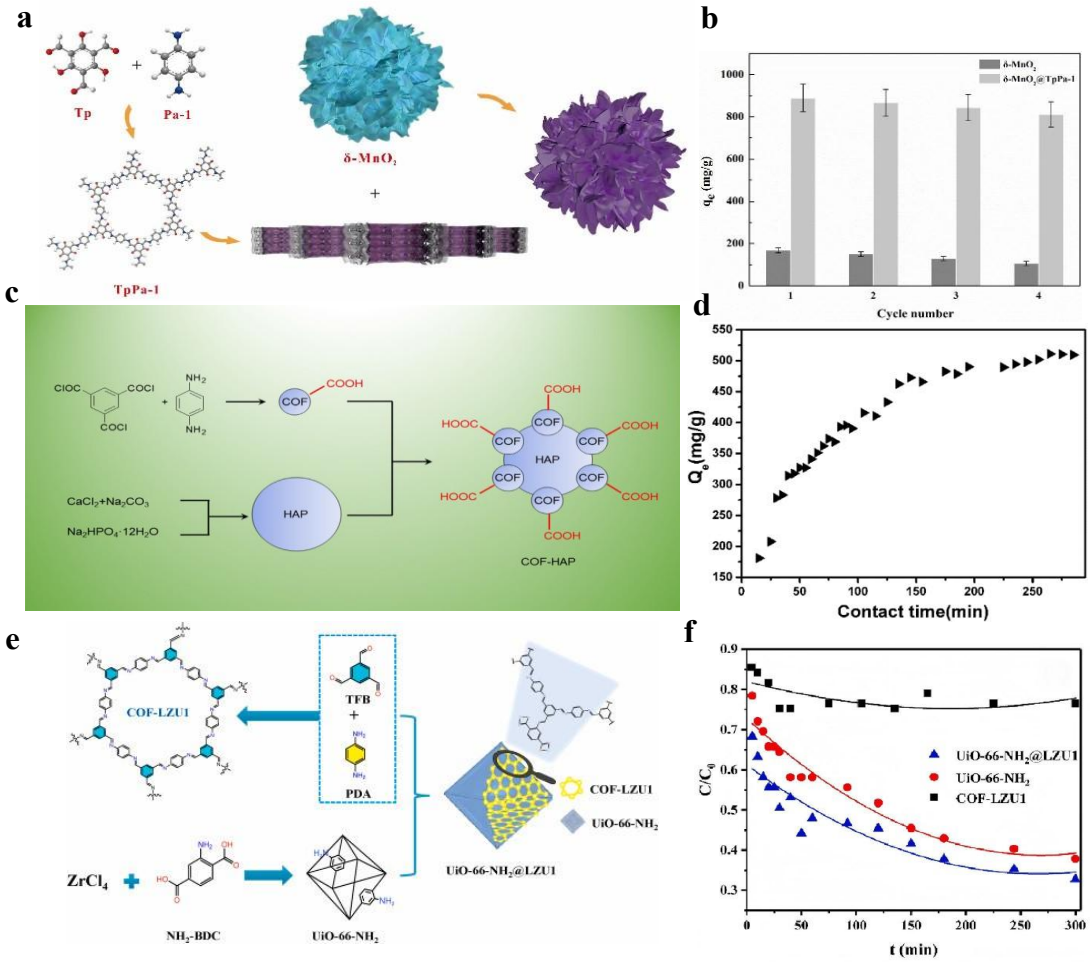

Figure 3. (a) The structural designs of δ-MnO_2@TpPa-1. (b) Adsorption-desorption cycles of U(VI) ion on δ-MnO_2 and δ-MnO_2@TpPa-1 [39]. (c) The flow chart of synthetic route to COF-HAP. (d) Effect of contact time on U(VI) adsorption [63]. (e) The synthesis process of UiO-66-NH_2@LZU1. (f) Effect of contact time on U(VI) adsorption onto COF-LZU1, UiO-66-NH_2 and UiO-66-NH_2@LZU1.

2.2. COFs for uranium from seawater under photocatalytic conditions

Semiconductor-based photocatalysis is a highly promising technology: it enables visible-light-driven chemical fuel production and environmental purification via pollutant photodegradation, prompting extensive efforts to develop stable, high-efficiency semiconductor catalysts.

2.2.1. Original COFs

Due to the complex marine systems, it is considered not only the large ion competition and ultra-low uranium concentration [64], but also the biological pollution problem encountered in the process of COFs application [65]. How to improve the biological pollution resistance of COFs has received wide attention. Cui et al. [66] conjugated naphthyl sp^2-carbon-COF (NDA-TN-AO) with excellent photocatalytic and optoelectronic properties, explored a new strategy for photoenhanced adsorption of uranium from natural seawater. Unlike biphenyl-based interrupted coupling, Cui et al. used naphthalene as a functional monomer. Since naphthalene has the full planar extended π-conjugated system [67], it can serve as a cornerstone for building semiconductor COFs with excellent photocatalytic properties. Excellent photocatalytic activity enables NDA-TN-AO to effectively destroy bacteria and biological entities by producing biotoxic reactive oxygen species (ROS), and promote photoelectrons to reduce adsorbed U(VI) to insoluble U(IV), thus significantly improving the extraction capacity of uranium (Figure 4a). Furthermore, the NDA-TN-AO surface produces a

large number of positive electrical holes. It has strong electrostatic attraction to soluble U(VI) in natural seawater and has high adsorption capacity. Since NDA-TN-AO can effectively generate biotoxic ROS, NDA-TN-AO can exhibit high anti to biological contamination performance by destroying the organic components. In this work, using bacteria as a model sample, Cui et al. NDA-TN-AO has high antimicrobial activity against a variety of tested strains (Figure 4b and 4c). SEM of V.alginolyticus after light irradiation showed that the entity was completely destroyed and its internal contents were released with no significant changes in the dark (Figure 4d). The above results show that NDA-TN-AO can effectively resist the biofouling of Marine bacteria. The adsorption experiments of NDA-TN-AO under light and dark irradiation were also carried out in uranium filtered and unfiltered natural seawater respectively (Figure 4e). Natural seawater was filtered by using a 0.22 μm sterile filter to remove bacteria. After filtration, NDA-TN-AO increased by 33 %, indicating that marine bacteria have a serious effect on NDA-TN-AO to uranium under dark conditions. However, the uranium adsorption of NDA-TN-AO increased by only 8.1 %, indicating that Marine bacteria had little effect on the uranium adsorption of NDA-TN-AO under light conditions. All these results prove that NDA-TN-AO has good photocatalytic and photoelectric activity (Figure 4f), which can photoenhance the adsorption of uranium in seawater.NDA-TN-AO is a renewable photocatalytic uranium adsorbent that still has a high elution rate (> 87 %) after six cycles (Figure 4g). Cui et al. measured adsorption capacity of NDA-TN-AO and BDA-TN-AO under simulated sunlight and dark conditions, NDATN-AO and BDA-TN-AO were 4.56 mg/g and 4.33 mg/g (Figure 4h). After 27 days of illumination, the uranium adsorption capacity of NDA-TN-AO increased by 33.0 %, which can be attributed to the better photocatalytic and photoelectric activity of NDA-TNAO. Both NDA-TN-AO and BDA-TN-AO showed selectivity for uranium and vanadium in seawater, but not for other metals (Figure 4i), consistent with the selectivity of the amidoxime group. Guo et al. [68] reported two COFs(r-i-COF1 and r-i-COF2) constructed by a liquid-solid two-phase strategy, reversibly and irreversibly, and found that this hybrid linked COF has excellent light-enhanced uranium extraction performance (Figure 5a). It was found that r-i-COF-1 and r-i-COF-2 had no adsorption capacity for uranium, and the extraction rate of cof under dark conditions was less than 4 % in a 10 ppm U(VI) solution. In contrast, the extraction efficiency of r-i-COF-1 under visible light irradiation was 19.8 % (Figure 5b), indicating that the photocatalytic effect was low due to the lack of strong electron transfer in r-i-COF-1. The extraction efficiency of r-i-COF-2 constructed by the strong electron-withdrawing monomer C under visible light irradiation was as high as 82.3 %, which is 4.1 times that of r-i-COF-1. It should be emphasized that such a high extraction efficiency in r-i-COF-2 is almost entirely due to photocatalysis, and the contribution of adsorption is negligible (only 4 %) (Figure 5c), and the photocatalytic uranium extraction capacity is increased by 64.2 times (Figure 5d). After five cycles of r-i-COF-2, the uranium extraction rate did not decrease significantly, indicating a good reuse. In addition, the selectivity for uranium is higher than that for the other 12 ions, with an extraction efficiency of uranium as high as 96.2 %, while the extraction efficiency for the other 12 metal ions is less than 5 % (Figure 5e).

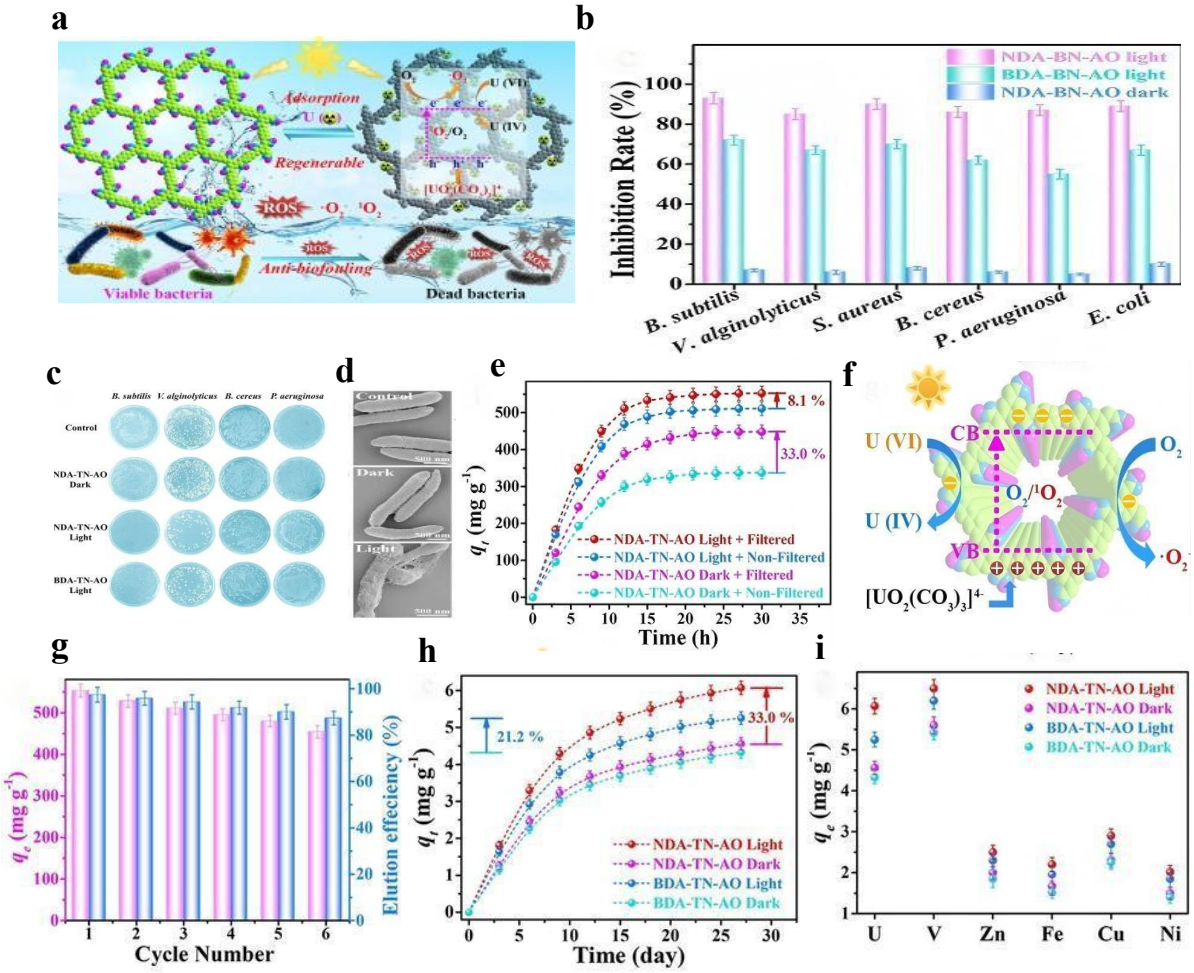

Figure 4. (a) Diagram of the construction of a highly planar conjugated COF adsorbent for photo-enhanced uranium adsorption from seawater. (b) Antibacterial activity. (c) Antibacterial spectrum. (d) SEM images of bacterial cells treated with NDA-TN-AO under light and dark conditions. (e) Effects of bacteria on uranium extraction capacity. (f) Proposed mechanism of NDA-TN-AO for the photo-enhanced uranium extraction. (g) The uranium adsorption capacity and elution efficiency of NDA-TN-AO. (h) Adsorption of uranium from seawater. (i) Selectivity of NDA-TN-AO and BDA-TN-AO for metals in seawater [66].

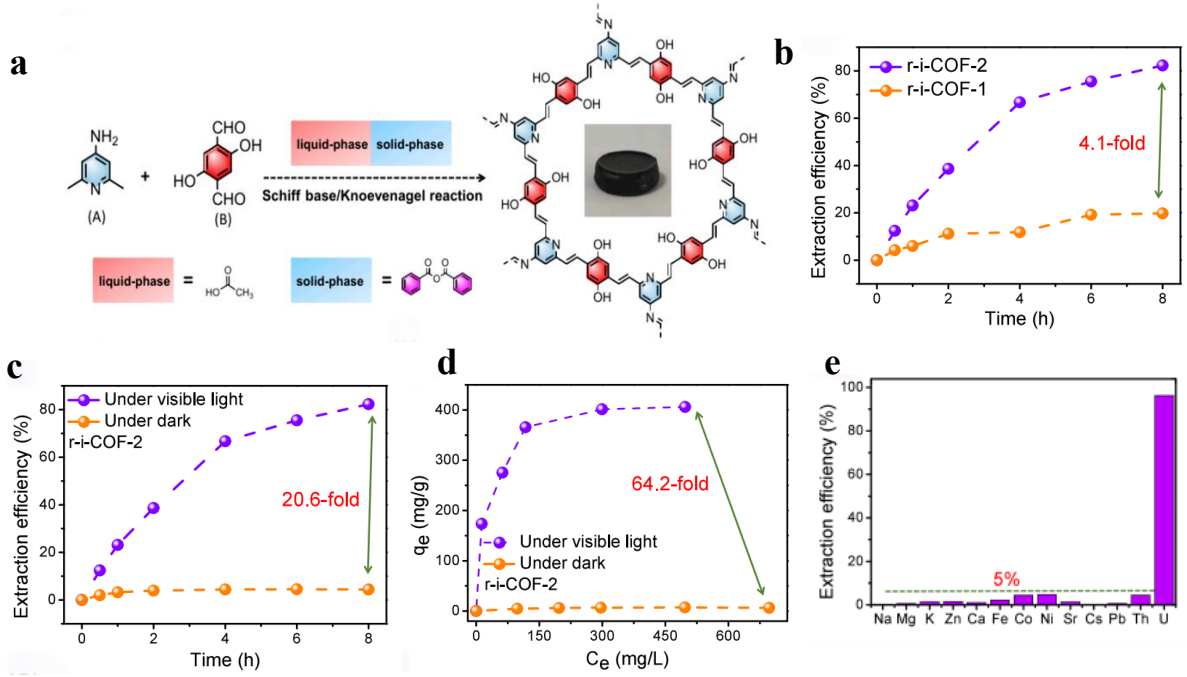

Figure 5. (a) Synthesis draft of r-i-COF-1. (b) Uranium extraction efficiency of r-i-COF-1 and r-i-COF-2 under visible light irradiation for a 10 ppm Uranium solution. (c) Uranium extraction efficiency of r-i-COF-2 under visible light irradiation and dark for a 10 ppm Uranium solution. (d) Uranium extraction capacity of r-i-COF-2 under visible light irradiation and dark. (e) Selective uranium extraction of r-i-COF-2 over other metal ions [68].

2.2.2. Functional group-modified COFs

The seawater environment is mostly a weakly alkaline environment, which enables the researchers to explore the materials that can extract uranium in the alkaline environment. Chen et al. [69] reported a strategy of a COFs photocatalytic material (TT-Por COF-Ni) to remove uranium in an alkaline solution at a non-sacrificial photocatalyst under air conditions. The material is a photocatalyst TT-por COF-Ni synthesized from an aldehyde amine reaction between TPP-Ni and TT (Figure 6a). This strategy generates hydrogen peroxide (H_2O_2) from photocatalytic reduction of O_2, and then reacts in situ with uranyl in situ to form subore (Figure 6b). The results show that in the air environment, this method can remove the residual uranium in the alkaline solution to 1 ppm, up to 83.1 % under the solar light (Figure 6c). The effect of pH on uranium removal rateshows that TT-Por COF-Ni acts as the photocatalyst, and the removal rate of uranium under alkaline conditions is higher than that under acidic conditions (Figure 6d). Chen et al. suggested that the solubility of subbodies and the generation of H_2O_2 are the two main factors affecting the uranium removal rate in solutions with different pH. Although H_2O_2 is less produced in alkaline solution than in acidic solution (Figure 6e) [70, 71] at lower pH. Therefore, the lower the pH is, the lower the removal rate of uranium. This indicates that TT-Por COF-Ni can better remove uranium in an alkaline environment, and most current photocatalysts are difficult to remove uranium because U(VI) is easily oxidized under alkaline conditions. Furthermore, the recyclable properties of the materials were explored, and the reacted photocatalyst was successively stirred in a saturated NH_4HCO_3 aqueous solution and 0.02 mol/L HCl for 12 hours [72]. The cleaned photocatalyst was dried in vacuum and used for the next step of photocatalytic uranium removal. After four cycles, the photocatalytic activity hardly decreased (Figure 6f), indicating that TT-Por COF-Ni has long-term photostability and can be recycled for at least 32 hours. Improving the selectivity and efficiency of COFs to recover uranium from seawater is a key aspect to be explored. To achieve this goal, Cui et al. [73] developed a series of strong and hydrophilic benzoxazole-based COFs (Tp-DBD, Bd-DBD, and Hb-DBD) respectively as efficient adsorbents for light-enhanced directional recovery of uranium (Figure 7a). Benefiting from the formation of hydroxyl and benzoxazole rings, Tp-DBD has excellent stability and chemical reduction

properties. The synergistic effect of the hydroxyl group and the benzoxazole ring in the π-conjugated framework significantly reduces the optical band gap and improves the affinity for uranium and the recovery ability. In the dark, Tp-DBD showed higher recovery ability than Tb-DBD, which may be because the introduction of hydroxyl groups improved the hydrophilicity of Tp-DBD, providing higher affinity and higher affinity for uranium binding. After simulated sunlight irradiation, the uranium recovery capacity of Tp-DBD increased by 53.9 %, from 653.9 mg/g to 1006.5 mg/g (Figure 7b). Light irradiation also shortened the equilibrium time from 9 h to 5 h, which may be due to the excellent photoelectric and photothermal effects that promote the conductivity and thermal motion of uranyl ions near Tp-DBD, thereby further enhancing the affinity of the binding site for uranium. In contrast, illumination has no significant effect on the uranium recovery capacity of Tb-DBD, and the uranium recovery capacity of Tp-DBD is 15.3 times higher than that of Tb-DBD under light conditions. The results show that the uranium recovery capacity of Tp-DBD is much higher than that of most porous framework materials. Moreover, due to the high affinity and selectivity of Tp-DBD for uranium, Tp-DBD has little adsorption of other metal ions, and the recovery capacity of uranium is 19.2 times that of vanadium (Figure 7c). Tp-DBD only showed an average 2.12 % decrease in uranium recovery capacity and an average 0.49 % decrease in the elution efficiency of each cycle after reused for ten times (Figure 7d). This performance is much higher than the strict commercial standard set by the economic evaluation of uranium recovery from seawater 3 % loss per cycle (Figure 7e).

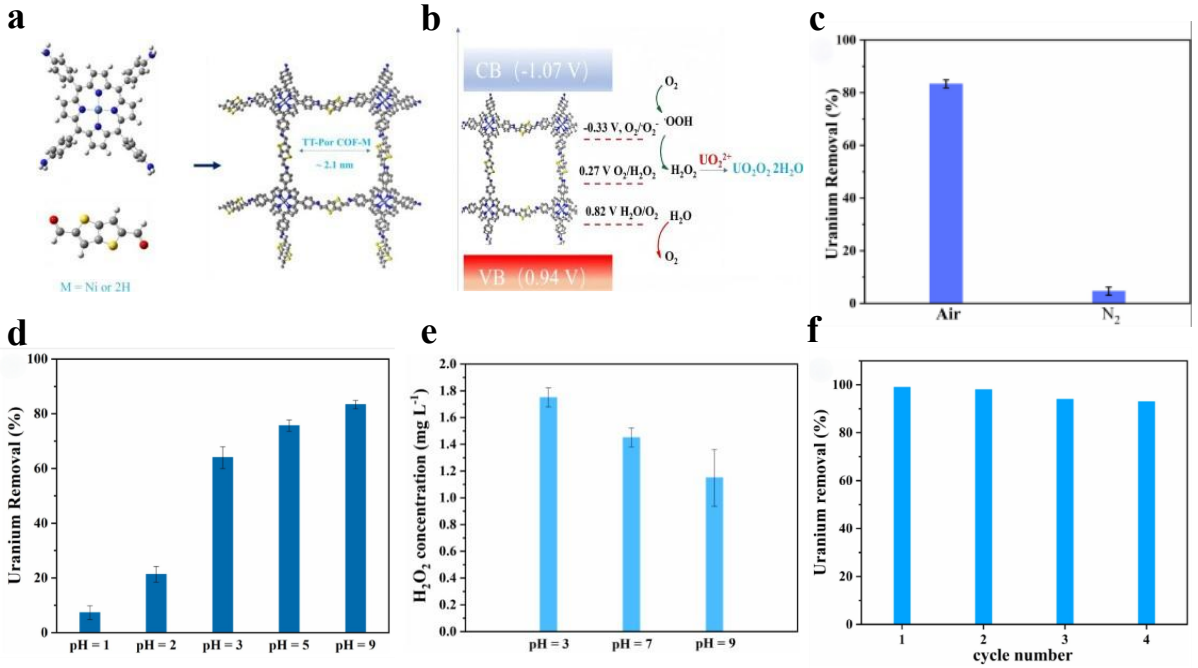

Figure 6. (a) Synthesis of the TT-Por COF-M. (b) Mechanism of H_2O_2 photosynthesis and uranyl removal. (c) Effect under air or N_2 atmosphere, C_0=200 ppm. (d) Effect of solution pH, C_0=200 ppm. (e) H_2O_2 photosynthesis under different pH values. (f) Recyclable performance of TT-Por COF-Ni, pH= 9, C_0=50 ppm [69].

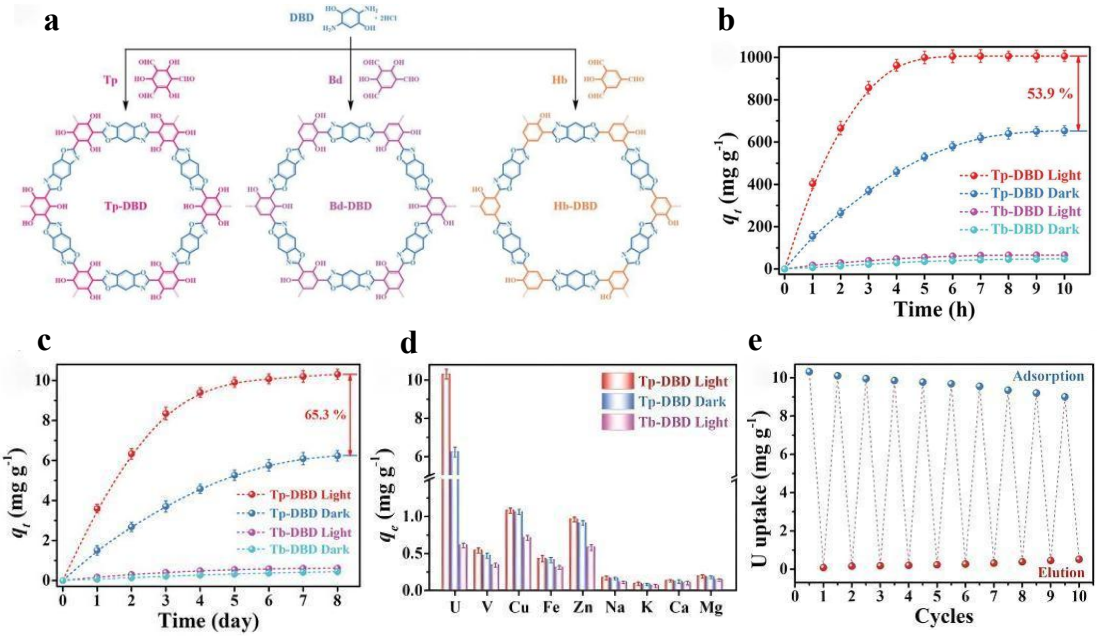

Figure 7. (a) Synthetic routes to Tp-DBD, Bd-DBD, and Hb-DBD. (b) Uranium recovery capacity of Tp-DBD and Tb-DBD under light and dark conditions. (c) Extraction of uranium from natural seawater. (d) Selectivity of Tp-DBD and Tb-DBD for metals in natural seawater. (e) Recycling experiment of the Tp-DBD under light irradiation conditions [73].

2.2.3. COFs combined with other materials

Liu et al. [55] synthesized a z-type van der Waals heterojunction photocatalyst (SnS_2COF) using COFs combined with a semiconductor (SnS_2) in situ. SnS_2COF has a wider light absorption range, more active sites, and higher separation and transfer efficiency of electrons (e^-) and holes (h^+). Therefore, it has a higher U(VI) reduction rate under UV/visible light. SnS_2COF removal rate of U(VI) was much higher than SnS_2 (343.6 mg/g) and COFs (485.4 mg/g), reaching 1123.3 mg/g (Figure 8a). The removal rate of SnS_2 physical mixing with COFs (SnS_2/COF) is only 378.8 mg/g. Thus, the enhanced performance enhancement of SnS_2COF is related to the formation of a heterojunction, during which photogenic e^- and h^+ holes also cross the heterogeneous interface, so that the in situ heterostructure facilitates electron transfer (Figure 8b). The adsorption amount of each catalyst in the dark was low, and the removal rate of U(VI) by SnS_2COF was about 15 %. However, the removal rate under light was close to 100 %, indicating that light is the key condition for SnS_2COF to reduce U(VI) (Figure 8c). Compared with SnS_2 and COFs, SnS_2COF removes U(VI) under light. In addition, Liu et al. found that different kinds of anions had little effect on the removal of U(VI), which was mainly attributed to the strong binding energy of the material on U(VI) (Figure 8d). More importantly, when the coexisting cation concentration is 5 times that of U(VI), the U(VI) removal rate is still higher than 95 % (Figure 8e). This proves that the material is suitable for extracting uranium in a wide variety of ions. Similar to two-dimensional materials such as graphene [74, 75] and the transition metal disulfide compound [76], the interlayer stacking structure of 2D-COFs not only affects structural features, such as crystallinity and porosity [77], but also determines its electronic and optical properties [78]. This plays an important role in the reduction of the U(VI) [79-82]. Gao et al. [83] used the same monomer to successfully synthesize two three-core COFs with different interlayer stacking structures: overlapping AA stacking in Cu_3-PA-COF-AA and staggered ABC stacking in Cu_3-PA-COF-ABC (Figure 9a). It is worth noting that various functions, including porosity, electronic and optical properties, can be effectively adjusted by interlayer stacking. The results showed that Cu_3-PA-COF-AA and Cu_3-PA-COF-ABC showed significant differences in photoreduction activities on U(VI), which provided a promising strategy for the U(VI) extraction in seawater. Photocatalytic activity was initially explored in U(VI) containing seawater (20 ppm) without any reagents at a solid-liquid ratio of 0.05 g/L. As shown in, Cu_3-PA-COF-AA had more

adsorption capacity than Cu_3-PA-COF-ABC (Figure 9b), but lower U(VI) removal rates in both. Under visible light irradiation, Cu_3-PA-COF-AA removed U(VI) sharply increased from 22.3 % to 93.6 %, which is about 2.2 times that of Cu_3-PA-COF-ABC (42.0 %), the U(VI) removal capacity in Cu3-PA-COF-AA reaches 375 mg/g (Figure 9c), showing excellent photocatalytic U(VI) removal rate. Additionally, the photocatalytic reduction activity of Cu_3-PA-COF-AA was explored under the N_2 atmosphere (Figure 9d), and the U(VI) removal ratio was further improved to 98.7 %. Moreover, after five catalytic cycles, the U(VI) removal rate in Cu_3-PA-COF-AA is almost the same as the initial value, indicating its excellent reusability (Figure 9e).

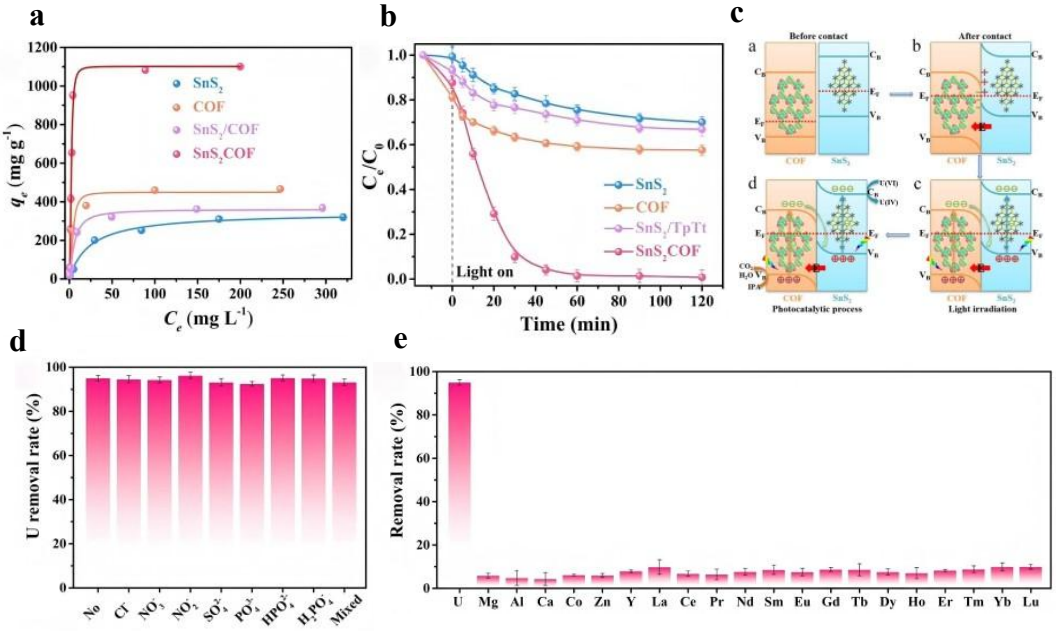

Figure 8. (a) Uranium removal isotherms of SnS_2, COF, SnS_2/COF, and SnS_2COF under light irradiation at pH=5.0. (b) Schematic diagram of the charge transfer process and photocatalytic mechanism of SnS_2COF heterojunction model. (c) The uranium removal rate of SnS_2, COF, SnS_2/COF, and SnS_2COF under light irradiation at pH=5.0. (d) Effect of different anions on U(VI) reduction by SnS_2COF. (e) Competitive removal of coexistent ions by SnS_2COF with concentration ratio of metal ions to U(VI) of about 5 times at pH=5.0 under UV/Vis light irradiation [55].

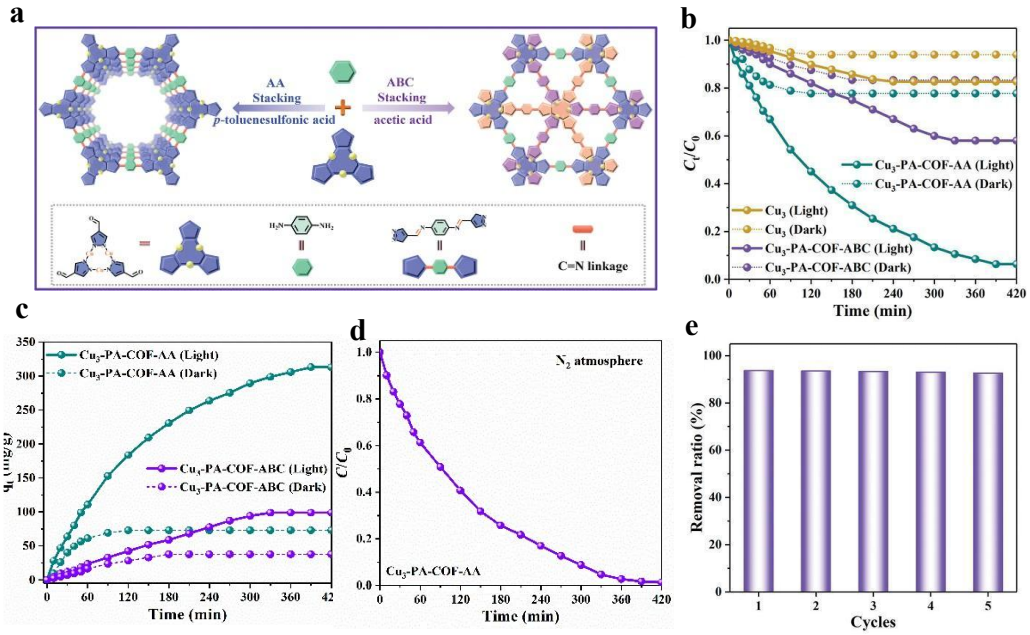

Figure 9. (a) Schematic representation for controllable synthesis of trinuclear copper organic framework with different interlayer stacking structures. (b) U(VI) removal ratio in the dark and upon visible-light irradiation. (c) U(VI) removal capacity with the initial concentration of ~20 ppm. (d) Removal ratio of Cu_3-PA-COF-AA under N_2 atmosphere. (e) U(VI) removal ratio of Cu_3-PA-COF-AA over five successive cycles [83].

3. CONCLUSIONS AND PERSPECTIVE

Seawater uranium extraction has emerged as a research hotspot in recent years, and this review summarizes the versatile roles of COFs in both adsorption and photocatalysis processes by virtue of their exceptional structural, large specific surface area, well-defined pores and tunable functional groups to extract U(VI) via physical adsorption or redox processes. Despite advances in improving U(VI) extraction capability, practical marine applications are hindered by multiple challenges: insufficient extraction efficiency, microbial interference and corrosion, limited scalability of lab-based synthesis methods, poor recyclability, secondary pollution risks from metal-containing COFs, and the lack of cost-effective large-scale fabrication approaches. To advance efficient, economical, and sustainable seawater uranium extraction, future efforts should prioritize: tailoring functional groups for stronger uranium affinity, optimizing pore structure to enhance adsorption capacity, improving environmental stability, developing regenerable COFs, integrating photocatalytic reduction technologies, and exploring scalable synthesis strategies.

REFERENCES

[1] Wang, Y., et al., Efficient recovery of uranium from saline lake brine through photocatalytic reduction. Journal of Molecular Liquids, 2020. 308.

[2] Xu, P., et al., Materials for lithium recovery from salt lake brine. Journal of Materials Science, 2020. 56(1): 16-63.

[3] Abney, C.W., et al., Materials for the Recovery of Uranium from Seawater. Chemical Reviews, 2017. 117(23): 13935-14013.

[4] Wang, Y., et al., Efficient recovery of uranium from saline lake brine through photocatalytic reduction. Journal of Molecular Liquids, 2020. 308.

[5] Xu, P., et al., Materials for lithium recovery from salt lake brine. Journal of Materials Science, 2020. 56(1): 16-63.

[6] Abney, C.W., et al., Materials for the Recovery of Uranium from Seawater. Chemical Reviews, 2017. 117(23): 13935-14013.

[7] Lindner, H., et al., Review of cost estimates for uranium recovery from seawater. Energy Economics, 2015. 49: 9-22.

[8] Singhal, P., et al., Magnetic nanoparticles for the recovery of uranium from sea water: Challenges involved from research to development. Journal of Industrial and Engineering Chemistry, 2020. 90: 17-35.

[9] Wang, Y., et al., Polyamidoxime-loaded biochar sphere with high water permeability for fast and effective recovery of uranium from seawater. Journal of Water Process Engineering, 2023. 55.

[10] Chen, T., et al., Advanced photocatalysts for uranium extraction: Elaborate design and future perspectives. Coordination Chemistry Reviews, 2022. 467.

[11] Lin, G., et al., A systematic review of metal organic frameworks materials for heavy metal removal: Synthesis, applications and mechanism. Chemical Engineering Journal, 2023. 460.

[12] Liu, X., et al., Metal-organic framework nanocrystal-derived hollow porous materials: Synthetic strategies and emerging applications. The Innovation, 2022. 3(5).

[13] Liu, Z., et al., Modified biochar: synthesis and mechanism for removal of environmental heavy metals. Carbon Research, 2022. 1(1).

[14] Yang, H., et al., Emerging technologies for uranium extraction from seawater. Science China Chemistry, 2022. 65(12): 2335-2337.

[15] Liu, T., et al., Photothermal enhancement of uranium capture from seawater by monolithic MOF-bonded carbon sponge. Chemical Engineering Journal, 2021. 412.

[16] Liu, W., et al., Highly Sensitive and Selective Uranium Detection in Natural Water Systems Using a Luminescent Mesoporous Metal-Organic Framework Equipped with Abundant Lewis Basic Sites: A Combined Batch, X-ray Absorption Spectroscopy, and First Principles Simulation Investigation. Environmental Science & Technology, 2017. 51(7): 3911-3921.

[17] Zheng, T., et al., Overcoming the crystallization and designability issues in the ultrastable zirconium phosphonate framework system. Nature Communications, 2017. 8(1).

[18] Wang, Z., et al., Constructing an Ion Pathway for Uranium Extraction from Seawater. Chem, 2020. 6(7): 1683-1691.

[19] Sun, Q., et al., Bio-inspired nano-traps for uranium extraction from seawater and recovery from nuclear waste. Nature Communications, 2018. 9(1).

[20] Yan, R. H., et al., Bio-inspired hydroxylation imidazole linked covalent organic polymers for uranium extraction from aqueous phases. Chemical Engineering Journal, 2021. 420.

[21] Zhang, L., et al., Skeleton Engineering of Homocoupled Conjugated Microporous Polymers for Highly Efficient Uranium Capture via Synergistic Coordination. ACS Applied Materials & Interfaces, 2019. 12(3): 3688-3696.

[22] Cui, W. R., et al., Regenerable and stable sp2 carbon-conjugated covalent organic frameworks for selective detection and extraction of uranium. Nature Communications, 2020. 11(1).

[23] Yang, H., et al., Functionalized Iron–Nitrogen–Carbon Electrocatalyst Provides a Reversible Electron Transfer Platform for Efficient Uranium Extraction from Seawater. Advanced Materials, 2021. 33(51).

[24] Cui, W. R., et al., Rational design of covalent organic frameworks as a groundbreaking uranium capture platform through three synergistic mechanisms. Applied Catalysis B: Environmental, 2021. 294.

[25] Jia, Z., et al., Metal-organic frameworks based mixed matrix membranes for pervaporation. Microporous and Mesoporous Materials, 2016. 235: 151-159.

[26] Wu, G., et al., Preparation of submicron PAF-56 particles and application in pervaporation. Microporous and Mesoporous Materials, 2019. 279: 19-25.

[27] Wu, G., et al., Tunable Pervaporation Performance of Modified MIL-53(Al)-NH2/Poly (vinyl Alcohol) Mixed Matrix Membranes. Journal of Membrane Science, 2016. 507: 72-80.

[28] Wu, G., et al., In situ preparation of COF-LZU1 in poly(ether-block-amide) membranes for efficient pervaporation of n-butanol/water mixture. Journal of Membrane Science, 2019. 581: 1-8.

[29] Jia, Z., et al., Amino-MIL-53(Al) sandwich-structure membranes for adsorption of p-nitrophenol from aqueous solutions. Chemical Engineering Journal, 2017. 307: 283-290.

[30] Luo, F., et al., A highly rare (3,4,5,6)-connected metal–organic framework containing three distinct Co2 secondary building units. Inorganic Chemistry Communications, 2010. 13(5): 671-675.

[31] Gao, Z., et al., Ultralow-Content Iron-Decorated Ni-MOF-74 Fabricated by a Metal–Organic Framework Surface Reaction for Efficient Electrocatalytic Water Oxidation. Inorganic Chemistry, 2019. 58(17): 11500-11507.

[32] Liu, L., et al., Rational design of MOF@COF composites with multi-site functional groups for enhanced elimination of U(VI) from aqueous solution. Chemosphere, 2023. 341.

[33] Afshari, M., et al., Synthesis of new imine-linked covalent organic framework as highly efficient absorbent and monitoring the removal of direct fast scarlet 4BS textile dye based on mobile phone colorimetric platform. Journal of Hazardous Materials, 2020. 385.

[34] Afshari, M., et al., Novel Triazine-Based Covalent Organic Framework as a Superadsorbent for the Removal of Mercury (II) from Aqueous Solutions. Industrial & Engineering Chemistry Research, 2020. 59(19): 9116-9126.

[35] Chen, X., et al., Covalent Organic Frameworks: Chemical Approaches to Designer Structures and Built-In Functions. Angewandte Chemie International Edition, 2019. 59(13): 5050-5091.

[36] Ding, S. Y., et al., Thioether-Based Fluorescent Covalent Organic Framework for Selective Detection and Facile Removal of Mercury (II). Journal of the American Chemical Society, 2016. 138(9): 3031-3037.

[37] Huang, N., et al., Stable Covalent Organic Frameworks for Exceptional Mercury Removal from Aqueous Solutions. Journal of the American Chemical Society, 2017. 139(6): 2428-2434.

[38] Huo, J., et al., Crystalline Covalent Organic Frameworks from Triazine Nodes as Porous Adsorbents for Dye Pollutants. ACS Omega, 2019. 4(27): 22504-22513.

[39] Li, X., et al., Function-oriented synthesis of two-dimensional (2D) covalent organic frameworks – from 3D solids to 2D sheets. Chemical Society Reviews, 2020. 49(14): 4835-4866.

[40] Liu, X., et al., Recent progress of covalent organic frameworks membranes: Design, synthesis, and application in water treatment. Eco-Environment & Health, 2023. 2(3): 117-130.

[41] Liu, X., et al., Advanced porous materials and emerging technologies for radionuclides removal from Fukushima radioactive water. Eco-Environment & Health, 2023. 2(4): 252-256.

[42] Zhong, X., et al., The fabrication of 3D hierarchical flower-like δ-MnO2@COF nanocomposites for the efficient and ultra-fast removal of UO22+ ions from aqueous solution. Environmental Science: Nano, 2020. 7(11): 3303-3317.

[43] Liu, X., et al., Surface nano-traps of Fe0/COFs for arsenic (III) depth removal from wastewater in non-ferrous smelting industry. Chemical Engineering Journal, 2020. 381.

[44] Yang, C. H., et al., Covalent organic framework EB-COF: Br as adsorbent for phosphorus (V) or arsenic (V) removal from nearly neutral waters. Chemosphere, 2020. 253.

[45] Chen, H., et al., Engineered biochar for environmental decontamination in aquatic and soil systems: a review. Carbon Research, 2022. 1(1).

[46] Lv, T. T., et al., Rapid and highly selective Sr2+ uptake by 3D microporous rare earth oxalates with the facile synthesis, high water stability and radiation resistance. Chemical Engineering Journal, 2022. 435: 134906.

[47] Yu, J., et al., Phosphonate-Decorated Covalent Organic Frameworks for Actinide Extraction: A Breakthrough Under Highly Acidic Conditions. CCS Chemistry, 2019. 1(3): 286-295.

[48] Jun, B. M., et al., Purification of uranium-contaminated radioactive water by adsorption: A review on adsorbent materials. Separation and Purification Technology, 2021. 278.

[49] Ma, H., et al., Radioactive Wastewater Treatment Technologies: A Review. Molecules, 2023. 28(4).

[50] Adamantiades, A. and I. Kessides, Nuclear power for sustainable development: Current status and future prospects. Energy Policy, 2009. 37(12): 5149-5166.

[51] Hao, M., et al., Modulating Uranium Extraction Performance of Multivariate Covalent Organic Frameworks through Donor–Acceptor Linkers and Amidoxime Nanotraps. JACS Au, 2023. 3(1): 239-251.

[52] Lei, J., et al., Progress and perspective in enrichment and separation of radionuclide uranium by biomass functional materials. Chemical Engineering Journal, 2023. 471.

[53] Mayer, K., et al., Uranium from German Nuclear Power Projects of the 1940s— A Nuclear Forensic Investigation. Angewandte Chemie International Edition, 2015. 54(45): 13452-13456.

[54] Wang, J., et al., Extraction and adsorption of U(VI) from aqueous solution using affinity ligand-based technologies: an overview. Reviews in Environmental Science and Bio/Technology, 2019. 18(3): 437-452.

[55] Li, Y., et al., Strategies for designing highly efficient adsorbents to capture uranium from seawater. Coordination Chemistry Reviews, 2023. 491.

[56] Endrizzi, F., et al., Chemical Speciation of Uranium (VI) in Marine Environments: Complexation of Calcium and Magnesium Ions with [(UO2) (CO3)3]4− and the Effect on the Extraction of Uranium from Seawater. Chemistry – A European Journal, 2014. 20(44): 14499-14506.

[57] Beltrami, D., et al., Recovery of Uranium from Wet Phosphoric Acid by Solvent Extraction Processes. Chemical Reviews, 2014. 114(24): 12002-12023.

[58] Liu, X., et al., SnS2-covalent organic framework Z-scheme van der Waals heterojunction for enhanced photocatalytic reduction of uranium (VI) in rare earth tailings wastewater. Chemical Engineering Journal, 2023. 460.

[59] Zhang, S., et al., "Stereoscopic" 2D super-microporous phosphorene-based covalent organic framework: Design, synthesis and selective sorption towards uranium at high acidic condition. Journal of Hazardous Materials, 2016. 314: 95-104.

[60] Zhang, J., et al., Construction of covalent organic framework with unique double-ring pore for size-matching adsorption of uranium. Nanoscale, 2020. 12(47): 24044-24053.

[61] Li, T., et al., Free testosterone value before radical prostatectomy is related to oncologic outcomes and post-operative erectile function. BMC Cancer, 2019. 19(1).

[62] Li, F. F., et al., Stable sp carbon-conjugated covalent organic framework for detection and efficient adsorption of uranium from radioactive wastewater. Journal of Hazardous Materials, 2020. 392.

[63] Zhang, C. R., et al., Simultaneous sensitive detection and rapid adsorption of UO22+ based on a post-modified sp2 carbon-conjugated covalent organic framework. Environmental Science: Nano, 2020. 7(3): 842-850.

[64] Li, J., et al., A novel benzimidazole-functionalized 2-D COF material: Synthesis and application as a selective solid-phase extractant for separation of uranium. Journal of Colloid and Interface Science, 2015. 437: 211-218.

[65] Sun, Q., et al., Covalent Organic Frameworks as a Decorating Platform for Utilization and Affinity Enhancement of Chelating Sites for Radionuclide Sequestration. Advanced Materials, 2018. 30(20).

[66] You, Z., et al., High Sorption Capacity of U(VI) by COF-Based Material Doping Hydroxyapatite Microspheres: Kinetic, Equilibrium and Mechanism Investigation. Journal of Inorganic and Organometallic Polymers and Materials, 2019. 30(6): 1966-1979.

[67] Yuan, Y., et al., Ultrafast Recovery of Uranium from Seawater by Bacillus velezensis Strain UUS-1 with Innate Anti-Biofouling Activity. Advanced Science, 2019. 6(18).

[68] Sulukan, E., et al., The synergic toxicity of temperature increases and nanopolystrene on zebrafish brain implies that global warming may worsen the current risk based on plastic debris. Science of The Total Environment, 2022. 808.

[69] Cui, W.R., et al., Regenerable Covalent Organic Frameworks for Photo-enhanced Uranium Adsorption from Seawater. Angewandte Chemie International Edition, 2020. 59(40): 17684-17690.

[70] Chen, R., et al., Designed Synthesis of a 2D Porphyrin-Based sp2Carbon-Conjugated Covalent Organic Framework for Heterogeneous Photocatalysis. Angewandte Chemie, 2019. 131(19): 6496-6500.

[71] Guo, L., et al., Linkage-Mixed Covalent Organic Frameworks Synthesized by a Liquid–Solid Two-Phase Strategy for Photoenhanced Uranium Extraction. Nano Letters, 2024. 24(32): 9854-9860.

[72] Chen, L., et al., Photocatalytic uranium removal from basic effluent by porphyrin-Ni COF as the photocatalyst. Chemical Engineering Journal, 2023. 454.

[73] Giménez, J., et al., Solubility study and point of zero charge of studtite (UO2O2·4H2O). Applied Geochemistry, 2014. 49: 42-45.

[74] Teng, Z., et al., Atomically dispersed antimony on carbon nitride for the artificial photosynthesis of hydrogen peroxide. Nature Catalysis, 2021. 4(5): 374-384.

[75] Zhou, D., et al., Cationic Effects on the Structural Dynamics of the Metal Ion–Crown Ether Complexes Investigated by Ultrafast Infrared Spectroscopy. The Journal of Physical Chemistry B, 2021. 125(46): 12797-12805.

[76] Cui, W.R., et al., Low Band Gap Benzoxazole-Linked Covalent Organic Frameworks for Photo-Enhanced Targeted Uranium Recovery. Small, 2021. 17(6).

[77] Novoselov, K. S., et al., Two-dimensional gas of massless Dirac fermions in graphene. Nature, 2005. 438(7065): 197-200.

[78] Cao, Y., et al., Unconventional superconductivity in magic-angle graphene superlattices. Nature, 2018. 556(7699): 43-50.

[79] Zhao, X., et al., Differentiating Polymorphs in Molybdenum Disulfide via Electron Microscopy. Advanced Materials, 2018. 30(47).

[80] Hmadeh, M., et al., New Porous Crystals of Extended Metal-Catecholates. Chemistry of Materials, 2012. 24(18): 3511-3513.

[81] Kuc, A., et al., Proximity Effect in Crystalline Framework Materials: Stacking-Induced Functionality in MOFs and COFs. Advanced Functional Materials, 2020. 30(41).

[82] Xiong, X. H., et al., Ammoniating Covalent Organic Framework (COF) for High-Performance and Selective Extraction of Toxic and Radioactive Uranium Ions. Advanced Science, 2019. 6(16).

[83] Li, Y., et al., Redox-Active Two-Dimensional Covalent Organic Frameworks (COFs) for Selective Reductive Separation of Valence-Variable, Redox-Sensitive and Long-Lived Radionuclides. Angewandte Chemie, 2020. 132(10): 4197-4204.